ISSN 1996-3343

Asian Journal of Applied Sciences

http://knowledgiascientific.com

Knowledgia SCIENTIFIC
A Place to Publish Outstanding Research

Asian Journal of Applied Sciences 2 (1): 83-90, 2009
ISSN 1996-3343

Electroless Ni-P Deposition on WE43 Magnesium Alloy Substrate

R. Azari Khosroshahi and N. Parvini Ahmadi
Faculty of Materials Engineering, Sahand University of Technology, Tabriz, Iran

Abstract: With the aim of study the nucleation and growth mechanism electroless Ni-P plating was applied to electrochemically heterogeneous WE43 magnesium alloy substrate. Experimental results revealed that the coating was preferentially nucleated on equilibrium β phase at along some grain boundaries and matrix dislocations. These were then spread to primary α phase. X-ray diffraction analysis of as deposited coatings showed a broad peak in the spectra, indicating an amorphous structure possibly with small microcrystalline areas. These were transformed to crystalline phase after annealing at temperatures 250 and 400°C for 1 h. Micro hardness testing results showed an increase in hardness from mean values of 650 Vickers for as plated samples to 960 and 1030 Vickers for the coated samples after annealing at 250 and 400°C for 1 h, respectively.

Key words: Magnesium alloy, electroless Ni-P coating, nucleation and growth mechanism

INTRODUCTION

The use of magnesium alloys in a variety of applications, particularly in aerospace, automobiles, mechanical and electronic components has increased steadily in recent years as magnesium alloys exhibit an attractive combination of low density, high strength-to-weight ratio, excellent castability, good mechanical and damping characteristics (Ambat and Zhou, 2004; Mordike and Ebert, 2001). WE43 (nominal composition in wt%: 4.1%Y-2.2%Nd-1%HRE-0.5%Zr) originally in the standard T6 condition (WE43-T6) is such an alloy which in addition to above mentioned properties, shows good creep behavior up to 300°C (Khosroshahi *et al*., 2006). However, magnesium is the least noble material with a potential of -2.34V vs. NHE (Normal Hydrogen Electrode). It has a high tendency to atmospheric and galvanic corrosion. In contrast to aluminum, magnesium does not form a self-heating passive surface. The reason is a misfit between hydroxide lattice [$Mg(OH)_2$] in the surface region and the lattice of the bulk material (Ferrando, 1989). Hence, the application of a suitable surface engineering technique is the most appropriate method to enhance the corrosion resistance of Mg based alloys. Among the various surface engineering techniques that are available for this purpose, coating by Electroless Nickel (EN) is of special interest due to the possession of a combination of properties, such as good corrosion and wear resistance, deposit uniformity, electrical and thermal conductivity and solderibility etc. (Gu *et al*., 2005; Liu and Gao, 2006). By the now there is very limited reports on EN plating on magnesium alloys, most of which are restricted to the magnesium based Al and Zn alloys (AZ series) and little information has been reported on WE43 or other Mg-RE alloys. The following paper reports our recent work on direct EN plating on WE43-T6 magnesium alloy with an attempt to understand the nucleation and growth mechanism of the deposit.

Corresponding Author: R. Azari Khosroshahi, Faculty of Materials Engineering, Sahand University of Technology, P.O. Box 51335-1996, Postal Code 53317-11111, Tabriz, Iran
Tel: +98-412-3459442 Fax: +98 412 344 4333

Table 1: Detailed sequences of EN operations

Stage No.	Constituent or condition		Value or range
1	Ultrasonic degreasing	Ethanol	5-10 min
2	Alkaline cleaning	NaOH	50 g L^{-1}
		Na_3PO_4	10 g L^{-1}
		Temperature	333±5 K
		Agitation	Mild, magnetic
		Time	8-10 min
3	Acid etching	CrO_3	125 g L^{-1}
	(Pickling)	HNO_3 (70% V/V)	110 ml L^{-1}
		Temperature	Ambient (293 K)
		Agitation	Vigorous, magnetic
		Time	30-60 sec
4	Fluoride activation	HF (40% V/V)	385 ml L^{-1}
		Temperature	Ambient (293 K)
		Time	10 min
5	Electroless nickel	Basic nickel carbonate	10 g L^{-1}
	Plating and operating	HF (40% V/V)	12 ml L^{-1}
	condition	Citric acid	5 g L^{-1}
		Ammonium bifluoride	10 g L^{-1}
		Sodium hypophosphite	20 g L^{-1}
		Ammonium hydroxide 25%	30 ml L^{-1}
		pH (colorimetric)	4.5-6.8
		Temperature	349-353 K
		Agitation required	Mild mechanical

MATERIALS AND METHODS

Rectangular coupons of 5×20×30 mm were cut from the supplied alloy WE43-T6 by Magnesium Electron Ltd. (MEL). The samples were mechanically polished with emery papers up to 1000 grit to ensure similar surface roughness. The polished substrates were thoroughly washed with distilled water before passing through the precleaning procedure.

Application of electrochemical plating on magnesium and its alloys requires surface pretreatment to ensure adhesion and integrity of the coatings. These steps include cleaning, etching and fluoride activation, followed in this case by EN plating. The detailed operation process is given in Table 1.

The deposition rate for plating on various substrates was measured from simple mass gains at the time intervals of 4, 6, 6.5, 7, 10, 20, 30, 60 and 110 min immersion. The microstructure of deposits and substrates were examined using a CamScan-Mv-2300 scanning electron microscopy equipped with an energy dispersive x-ray analysis (EDX). The structure of the deposits was determined before and after heat treatment by a Bruker-D8 advanced x-ray diffractometer with Cu-K_α radiation. The micro-hardness of EN coatings was also measured using a diamond indenter. Vickers hardness values were obtained by averaging five measurements on each specimen with an applied load of 50 g.

RESULTS AND DISCUSSION

Surface Pretreatment

Scanning electron microscopy of the alloy at various precleaning stages is shown in Fig. 1. According to the figure ultrasonic degreasing and alkaline cleaning do not influence surface roughness of the alloy, but etching by a chromic acid plus nitric acid solution makes the specimen surface rougher, which improves the adhesion of the coatings and makes the surface more chemically active (Gray and Luan, 2002). Similarly, after proper fluoride activation, we found that the substrate surface does not appear to be significantly different from the chemically etched one. Fluoride activation gives rise to the formation of MgF_2 film on the substrate surface which causes the nucleation rate to increase and a compact deposit to be achieved (Lian *et al*., 2006).

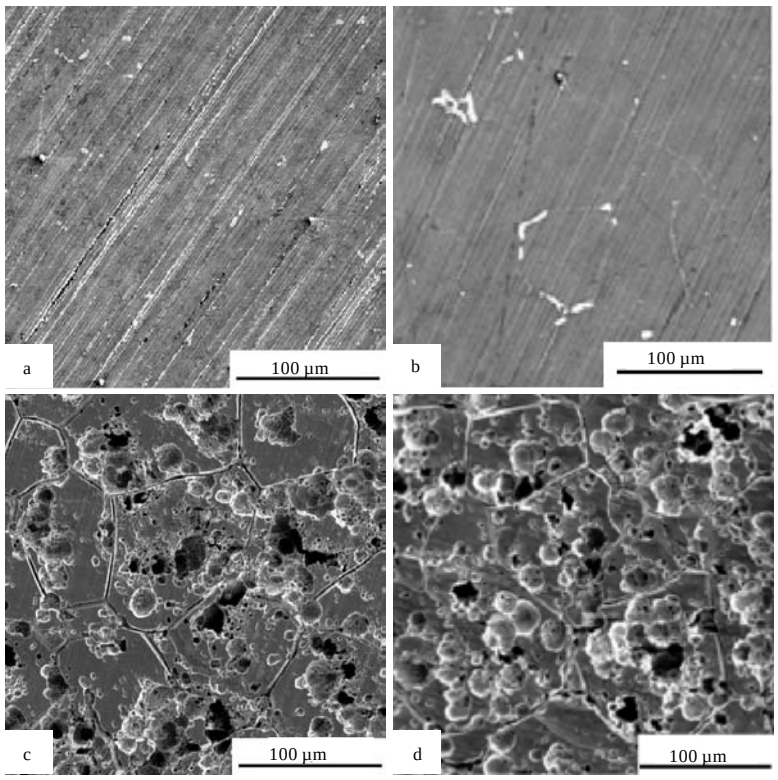

Fig. 1: SEM micrographs of the alloy at various precleaning stages

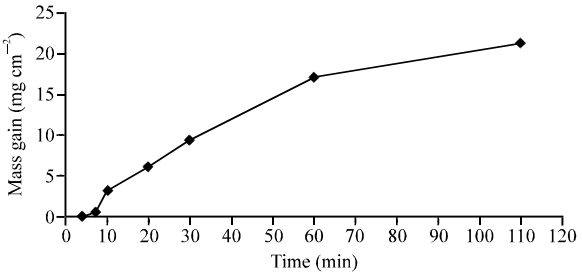

Fig. 2: Variation in deposition mass gain as a function of plating time

Deposition Rate and Deposit Morphology

Figure 2 shows the variation in deposition mass gain as a function of time at constant temperature and pH on WE43-T6 substrate. According to the figure at the early stages of coating, the deposition rate is low and the mass gain curve does not follow a linear relation with time as reported by some references, but agreed with other reports (Sharma *et al*., 1998) and consists of three stages: an initial stage about 0 to 10 min when the deposition rate was very low, followed by an acceleration period with a high and constant deposition rate up to 60 min and a third period with a slowly decreasing deposition rate. The early stages of the mass gain curve can be resulted from simple replacement

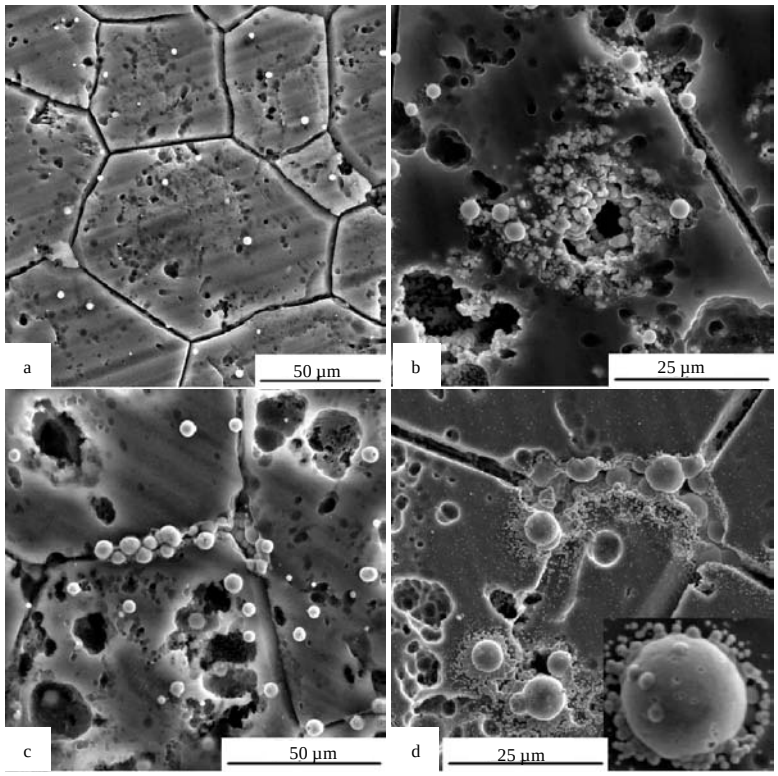

Fig. 3: Early stages of coating at time intervals of (a) 4, (b) 6, (c) 6.5 and (d) 7 min

reaction of nickel with magnesium at this stage. While the linear stage of the curve can be explained by the autocatalytic reaction theory in a perfect state, many significant factors may influence initial deposition mechanism such as the substrate surface roughness and chemical states. Figure 3 shows the early stages of coating at the time intervals of 4, 6, 6.5 and 7 min. According to the figure the EN deposits are preferentially nucleated on matrix corroded areas and/at along some grain boundaries. These were then spread mainly by deposition of new nuclei around primary ones. The extension mechanism of the nuclei is shown as the inset in Fig. 3d.

The microstructure of the alloy WE43-T6 consisted of equiaxed grains (α phase) together with homogeneously distributed intermetallic β" precipitates with a $D0_{19}$ ordered hexagonal crystal structure and β' precipitates with a base centered orthorhombic crystal structure. Some heterogeneously distributed β precipitates with a face centered cubic structure were also observed on matrix dislocations and along some grain boundaries (Khosroshahi *et al*., 2006).

The results of the present study revealed that the EN deposits were preferentially nucleated on the β phase at matrix dislocations (corroded areas in Fig. 3b, c) within the grains and along some grain boundaries (Fig. 3c, d), probably due to the galvanic coupling between β and primary α phases. In fact the electrons produced by the anodic dissolution from the α-phase are consumed by the cathodic deposition of EN on the β-phase or the adjacent sites, which may be treated as a type of replacement reaction. The formation of galvanic cells between β-$Mg_{17}Al_{12}$ phase (with free corrosion potential of nearly -1.0 V) and matrix α-phase (with free corrosion potential of -1.73 V) in AZ91 alloy (Huo *et al*., 2004) and preferential nucleation of EN on β-$Mg_{17}Al_{12}$ phase have been reported elsewhere

(Ambat and Zhou, 2004; Xiiang *et al*., 2001). It has been reported that the addition of rare earth elements such as Nd, La and Ce to magnesium leads the corrosion resistance of the alloy to be improved (Takenaka *et al*., 2007). Microstructural studies of the WE43-T6 alloy revealed that the most amount of alloying elements segregate to β phase (Khosroshahi *et al*., 2006) resulting in a non-uniform potential across the substrate.

At the site of α phase, Mg is dissolved as Mg^{+2} in the solution:

$$Mg = Mg^{2+} + 2e \tag{1}$$

At the β phase, the electrons produced from Eq. 1 are consumed for the reduction of nickel ions at the beginning of the plating process:

$$Ni^{2+} + 2e = Ni \tag{2}$$

After initial stage of nucleation, the second stage with a high and constant deposition rate begins and prolongs up to 60 min. Extension of nucleation at this stage can be explained by the autocatalytic reaction theory. It is predicted from Fig. 2 and the inset in Fig. 3d that autocatalytic reaction should play more important role after 10 min nucleation on WE43-T6 substrate which may explain why EN deposition mass gain increases rapidly after 10 min plating. In fact during nucleation at the early stages of plating the Ni crystallites act as catalytic sites to absorb hydrogen atoms and the autocatalytic reaction for EN deposition was initiated by dehydrogenation of the reducing agent (Liu and Gao, 2006). Thus the new nuclei begin to form adjacent to stable Ni crystallites and extend to the α phase (inset in Fig. 3d). Several mechanisms have been proposed for the chemical reactions which occur in hypophosphite-reduced EN plating solutions. The most widely accepted mechanism is illustrated through the following equations:

$$(H_2PO_4)^- + H_2O \rightarrow H^+ + (HPO_3)^{2-} + 2H_{abs} \tag{3}$$

$$Ni^{2+} + 2H_{abs} \rightarrow Ni + 2H^+ \tag{4}$$

$$(H_2PO_2)^- + H_{abs} \rightarrow H_2O + OH^- + P \tag{5}$$

$$(H_2PO_2)^- + H_2O \rightarrow H^+ + (HPO_3)^{2-} + H_2 \tag{6}$$

In the presence of a catalytic surface and sufficient energy, hypophosphite ions are oxidized to orthophosphate. A portion of the hydrogen given off is absorbed onto the catalytic surface (Eq. 3). Nickel at the surface of the catalyst is then reduced by the absorbed active hydrogen (Eq. 4). Simultaneously, some of the absorbed hydrogen reduces a small amount of the hypophosphite at the catalytic surface to water, hydroxyl ion and phosphorus (Eq. 5). Most of the hypophosphite present is catalytically oxidized to orthophosphate and gaseous hydrogen (Eq. 6) independently of the deposition of nickel and phosphorus, causing the low efficiency of electroless nickel solutions.

Examination of the surface morphology of the coated samples revealed that, plating for 30 min has not given rise to a defect free deposit (Fig. 4a). This was gradually changed to a compact and optically smooth morphology with an amorphous and/microcrystalline structure when plating time was increased to 60 min (Fig. 4b). Figure 5 shows the cross section of the EN deposit on the alloy

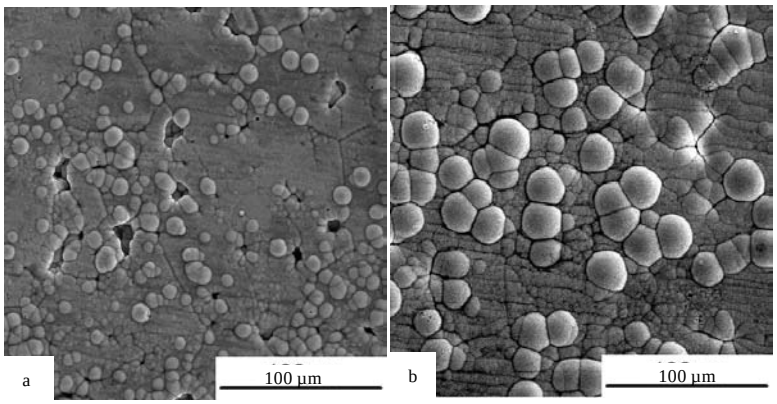

Fig. 4: Surface morphology of EN coated samples for times (a) 30 and (b) 60 min

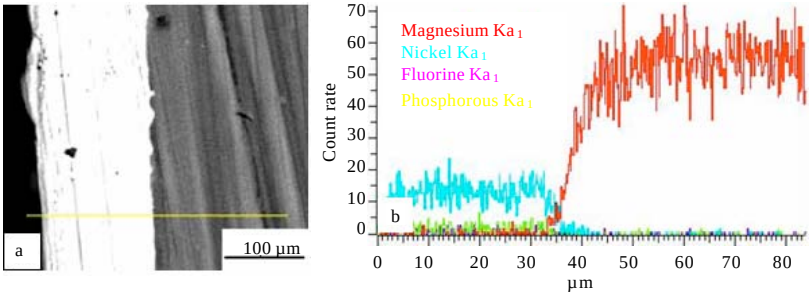

Fig. 5: Cross section of the (a) EN deposited alloy and (b) compositional variations along the indicated line

together with the compositional variations along the line (line scan) shown on Fig. 5a. The coating has a good adhesion to the substrate and no cracks or holes were observed. Continuing coating process for more than 60 min resulted in a gradual decrease in EN deposition rate (Fig. 2). The morphology of the deposit after 110 min plating time was found to be the same as that of plated for 60 min, but the more plating time gave rise to slightly thicker deposits. Decrease in deposition rate in stage 3 can be probably due to reduction in the concentration of hypophosphite ions in the solution as coating proceeds. The same observation has been reported by Lia and Gao when they studied the EN plating on some magnesium based Al (AZ series) substrates (Liu and Gao, 2006).

Annealing Treatment of EN Deposited Alloy

X-ray diffraction patterns of the EN coated samples before and after annealing at temperatures 250 and 400°C for 1 h are shown in Fig. 6. In the as-deposited condition there is a single broad peak around 2θ of 45° indicative of the amorphous/microcrystalline nature of the deposit. Annealing at 250°C for 1 h changes the nature of the deposit and more Ni peaks at higher angles as well as Ni_3P peaks are appeared in the diffraction patterns due to the crystallization process. Annealing at 400°C gave rise to the same but slightly sharper peaks (Fig. 6) belonging to the Ni and Ni_3P phases in the pattern.

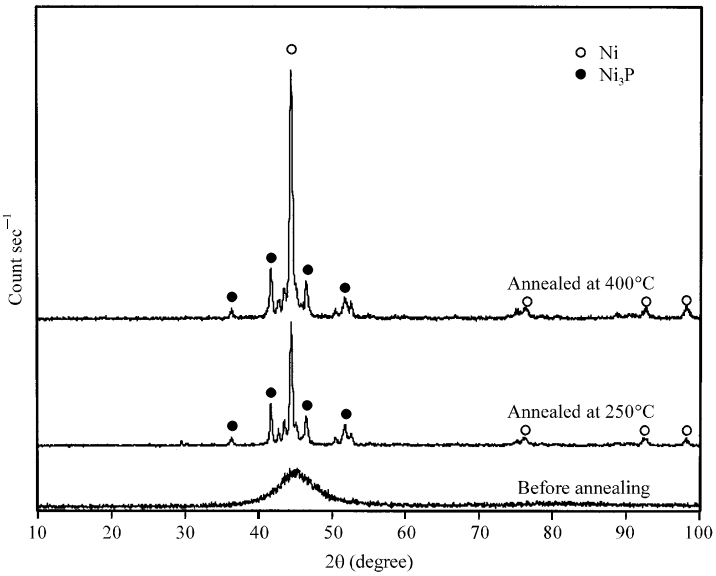

Fig. 6: X-ray diffraction patterns of the EN coated samples before and after annealing at 250 and 400°C for 1 h

Table 2: Hardness values of EN coating

Condition	Uncoated substrate	As-plated deposit	Annealed deposit at 250°C	Annealed deposit at 400°C
Hardness (VHN)	95	630	960	1030

Mean microhardness values of the uncoated alloy and EN deposits before and after annealing at 250 and 400°C for 1 h are shown in Table 2. As indicated the hardness of the as coated alloy is about 650 VHN, which is considerably higher than of the uncoated alloy substrate (about 95 VHN). This was further increased to about 960 VHN and 1030 VHN when EN deposits were annealed at 250 and 400°C for 1 h, respectively. This was found to be due to the formation of crystalline phases which takes place during annealing treatments.

The heat treated deposits at 400°C for 1 h showed slightly higher hardness values as compared to those of heat treated at 250°C. This is believed to be mainly due to higher volume fraction of crystalline phases formed at 400°C than 250°C. An increase in hardness values of EN deposits on an AZ91D alloy from 850 to 990 VHN as a result of increase in annealing temperature from 230 to 400°C has been reported elsewhere (Anik and Korpe, 2007).

CONCLUSIONS

- Substrate surface roughness was significantly increased as a result of chemical pretreatment before plating process.
- It was found that EN deposition was preferentially initiated on the β phase at dislocations within the grains and along some grain boundaries due to the galvanic coupling effect. These were subsequently extended with a high and constant deposition rate by the autocatalytic reaction mechanism.
- X-ray diffraction studies revealed an amorphous nature for the deposits before heat treatment process. This was changed to a crystalline structure consisted of Ni and Ni_3P phases as a result of annealing treatment at 250 and 400°C for 1 h.

- The hardness values of the uncoated alloy were significantly increased after EN coating process. These were further increased when the deposits were annealed at 250 and 400°C for 1 h. The heat treated deposits at 400°C showed slightly higher hardness values than those of heat treated at 250°C due to higher volume fraction of crystalline phases formed at higher temperature.

ACKNOWLEDGMENT

The authors wish to express their thanks for supporting this research by Sahand University of Technology.

REFERENCES

Ambat, R. and W. Zhou, 2004. Electroless nickel plating on AZ91D magnesium alloy: Effect of substrate, microstructure and plating parameters. Surf. Coat. Technol., 179: 124-134.

Anik, M. and E. Korpe, 2007. Effect of alloy microstructure on electroless Ni-P deposition behavior on alloy AZ91. Surf. Coat. Technol., 201: 4702-4710.

Ferrando, W.A., 1989. Review of corrosion and corrosion control of magnesium alloys and composites. J. Mater. Eng., 11: 299-313.

Gray, J.E. and B. Luan, 2002. Protective coatings on magnesium and its alloys-a critical review. J. Alloys Compounds, 336: 88-113.

Gu, C., J. Lian, G. Li, L. Niu and Z. Jiang, 2005. Electroless Ni-P plating on AZ91D magnesium alloy from a sulfate solution. J. Alloys Compounds, 391: 104-104.

Huo, H., Y. Li and F. Wang, 2004. Corrosion of AZ91D magnesium alloy with a chemical conversion coating and electroless nickel layer. Corrosion Sci., 46: 1467-1467.

Khosroshahi, R.A., N. Parvini Ahmadi and A. Torabadi, 2006. Study on chloridic corrosion of two magnesium alloys WE43 and WE54. In: Proceedings of the 7th International Conference on Magnesium Alloys and Their Applications. Kainer, Dresden, Germany, ISBN-13: 978-3-527-31764-6, ISBN-10: 3-527-31764-3 pp: 796-801.

Lian, J.S., G.Y. Li, L.Y. Niu, C.D. Gu, Z.H. Jiang and Q. Jiang, 2006. Electroless Ni-P deposition plus zinc phosphate coating on AZ91D magnesium alloy. Surf. Coat. Technol., 200: 5956-5962.

Liu, Z. and W. Gao, 2006. The effect of substrate on the electroless nickel plating of magnesium and magnesium alloys. Surf. Coat. Technol., 200: 3553-3560.

Mordike, B.L. and T. Ebert, 2001. Magnesium: Properties-applications-potential. Mater. Sci. Eng. A, 302: 37-45.

Sharma, A.K., M.R. Suresh, H. Bhojraj and H. Narayanamurthy, 1998. Electroless nickel plating on magnesium alloy. Metal Finishing, 96: 10-16.

Takenaka, T., T. Ono, Y. Narazaki, Y. Naka, M. Kawakamiakenaka, T. Ono, Y. Narazaki, Y. Naka and M. Kawakami, 2007. Improvement of corrosion resistance of magnesium metal by rare earth elements. Electrochimica Acta, 53: 117-121.

Xiiang, Y., W. Hu, X. Liu, C. Zhao and W. Ding, 2001. Initial deposition mechanism of electroless nickel plating on magnesium alloys. Trans. Inst. Met. Finish. (UK), 79: 30-32.